

Geophysical Research Letters*

L

RESEARCH LETTER

10.1029/2023GL104210

Kev Points:

- The Nonhydrostatic Icosahedral Atmosphere Model well reproduces observed spatiotemporal distributions of tropical overshooting deep convections (ODCs)
- Tropical ODC increases with global temperature on ocean (land) by 7%/K (-1%/K) for ODCs above 15.5 km, 27%/K (10%/K) above 16.9 km, and 90%/K (37%/K) above 18.4 km
- Response of tropical ODCs that penetrate the tropical cold point tropopause height to global warming is 3%/K, with 6%/K over the ocean and -3%/K on land

Correspondence to:

Q. Fu, qfu@atmos.washington.edu

Citation:

Wu, X., Fu, Q., & Kodama, C. (2023). Response of tropical overshooting deep convection to global warming based on global cloud-resolving model simulations. *Geophysical Research Letters*, 50, e2023GL104210. https://doi. org/10.1029/2023GL104210

Received 19 APR 2023 Accepted 12 JUL 2023

Author Contributions:

Conceptualization: Xueke Wu, Qiang Fu
Data curation: Chihiro Kodama
Formal analysis: Xueke Wu
Funding acquisition: Xueke Wu
Methodology: Xueke Wu, Qiang Fu
Software: Xueke Wu
Supervision: Qiang Fu
Validation: Chihiro Kodama
Visualization: Xueke Wu
Writing – original draft: Xueke Wu,
Qiang Fu, Chihiro Kodama

© 2023 The Authors.

This is an open access article under the terms of the Creative Commons Attribution-NonCommercial License, which permits use, distribution and reproduction in any medium, provided the original work is properly cited and is not used for commercial purposes.

Response of Tropical Overshooting Deep Convection to Global Warming Based on Global Cloud-Resolving Model Simulations

Xueke Wu¹, Qiang Fu², and Chihiro Kodama³

¹College of Atmospheric Sciences, Key Laboratory for Semi-Arid Climate Change of the Ministry of Education, Lanzhou University, Lanzhou, China, ²Department of Atmospheric Sciences, University of Washington, Seattle, WA, USA, ³Japan Agency for Marine-Earth Science and Technology, Yokohama, Japan

Abstract Tropical overshooting deep convections (ODCs) play a vital role in vertical transport of boundary layer pollutants, especially short-lived species, to upper troposphere and lower stratosphere, with important implications for stratospheric ozone and climate. We use simulations from a global cloud-system resolving model, Nonhydrostatic Icosahedral Atmosphere Model (NICAM), to study ODC changes from historical period to the end of the 21st century. NICAM well reproduces Tropical Rainfall Measuring Mission-satellite observed ODC spatiotemporal patterns. The future occurrences of ODCs with cloud top height above 15.5, 16.9, and 18.4 km scaled by the global temperature increase will increase by 7%/K, 27%/K, and 90%/K, respectively, over ocean where the atmosphere is becoming warmer and wetter. The corresponding changes are -1%/K, 10%/K, and 37%/K over land where the atmosphere will become hotter but drier. Relative to tropical cold point tropopause height, ODCs will only change by 3%/K, with 6%/K over the ocean but -3%/K on land.

Plain Language Summary Tropical overshooting deep convection (ODC) plays an important role in transporting short-lived chemical species rapidly from troposphere to stratosphere. This study shows that the simulations from a global cloud-system resolving model, Nonhydrostatic Icosahedral Atmosphere Model (NICAM), can well capture observed spatiotemporal variations of tropical ODCs. The NICAM simulations predict that by the end of the 21st century (2075–2104) versus the historical period (1979–2008) with a global-mean surface air temperature increase of 2.67 K, ODC occurrences with cloud tops reaching above 15.5, 16.9, and 18.4 km will increase by 14%, 59%, and 189%, respectively. Thus ODCs with higher cloud tops increase by a larger fraction than ODCs with lower cloud tops. The corresponding changes in ODC occurrences over the future warmer (hotter) and wetter (drier) oceanic (terrestrial) environments will be 20% (–2%), 72% (27%), and 240% (98%). Thus ODCs over ocean generally increase at a faster rate than over land. With tropical cold point tropopause height as a reference level, which will increase from 17.2 to 18.1 km, ODCs will increase by only 8% over the tropics, with 15% over ocean but decrease by –8% over land.

1. Introduction

Climate change due to increases of greenhouse gas concentrations has led to a substantial increase in intense convection (e.g., C. Liu, 2017; Taylor et al., 2017) and extreme precipitation (e.g., Donat et al., 2016; Min et al., 2011). In addition to being an important component of the global hydrological and energy cycles, the tropical overshooting deep convection (ODC) has been proven to be prominent in transporting moisture and pollutants to the tropical tropopause layer (TTL) between ~14.5 and 18.5 km (Fu et al., 2007; Fueglistaler et al., 2009). This exerts a disproportionate and profound impact on the thermodynamics and chemical composition of the TTL (e.g., Kuang & Bretherton, 2004; Takahashi & Luo, 2014). Although the effect of ODCs on stratospheric-tropospheric exchange of moisture (i.e., dehydration vs. hydration) is still a subject of debate (e.g., Frey et al., 2015; Kuang & Bretherton, 2004; Küpper et al., 2004), the ODCs play an indisputable role in transporting short-lived chemical species rapidly from the troposphere to the TTL (Bergman et al., 2012; Frey et al., 2015; Pan et al., 2017). The ODCs can also transport lightning-produced nitrogen oxides and hydroxyl radicals from middle and upper troposphere to the TTL and even directly into the lower stratosphere. However, most previous studies are on case studies of convective transports while the climatology of the extent and occurrence frequency of tropical ODCs and especially their future changes receives less attention (e.g., Aumann et al., 2018; Chaboureau et al., 2007; Fan et al., 2010; Grosvenor et al., 2007; Takahashi & Luo, 2014).

WU ET AL. 1 of 10

Global climate models (GCMs) are a major tool for studying future climate change including extreme precipitation (i.e., Ban et al., 2015; L. Lin et al., 2016, 2018; O'Gorman & Schneider, 2009; Tong et al., 2022), severe storms (e.g., Del Genio et al., 2007), and lightning (Finney et al., 2014; Romps et al., 2014). It is predicted that extreme precipitation and the most severe storms will increase (e.g., Bao et al., 2017) and intensify (O'Gorman, 2015) in a warmer climate. Unfortunately, the future change of global tropical ODCs due to global warming is not well documented. One key limitation of current GCMs is that convection is parameterized, which is not ideal for predicting the future changes of convection-related extreme events. On the other hand, cloud-resolving models (CRMs) have proven capable of reproducing convection-related precipitation, CAPE, and severe storms (e.g., Romps, 2019), but have mainly been used for regional rather than global long-term simulations.

In recent years, global cloud-resolving models (GCRMs) have been used to explicitly resolve moist convection in the global dynamics context without using cumulus parameterization (e.g., Satoh et al., 2019). With the rapid advances in GCRMs and computing power, it has become possible for us to better document and understand the response of deep convection to climate change on the global scale (e.g., Na et al., 2020). The Nonhydrostatic Icosahedral Atmosphere Model (NICAM) (Satoh et al., 2008, 2014; Tomita & Satoh, 2004) is designed to conduct global deep convection simulation without cumulus parameterization. Herein the NICAM long-term simulations in both historical (1979–2008) and future conditions (2075–2104) with a 14-km resolution are employed to investigate the extent, number, and future characteristics of tropical ODCs. The Tropical Rainfall Measuring Mission (TRMM) satellite observations of ODCs from 1998 to 2013 are used to evaluate the NICAM-simulated ODCs. Section 2 describes the data and methods used in this study. The comparison of NICAM-simulated ODCs with TRMM observation is presented in Section 3, and the future changes in ODCs are shown and discussed in Section 4. The conclusions are given in Section 5.

2. Data and Methods

The NICAM is based on a nonhydrostatic equation system and a quasi-uniform grid mesh structure (Satoh et al., 2008, 2014; Tomita & Satoh, 2004). It has been shown to reproduce a realistic multiscale cloud structure from the mesoscale to the planetary-scale, at a horizontal resolution between 14 and 3.5 km (Miura et al., 2007; Na et al., 2022; Tomita et al., 2005). We use the climate simulation from the NICAM.12 version (Kodama et al., 2015; Satoh et al., 2015) for both the historical period of 1979–2008 and the future period of 2075–2104 with the Intergovernmental Panel on Climate Change A1B emission scenario. These simulations were performed with a horizontal resolution of 14 km and 38 vertical layers up to 40 km. The NICAM simulations with a 14-km horizontal resolution without cumulus parameterization have been shown to be able to reproduce the multiscale structure of convective systems embedded in super-cloud clusters, Madden Julian Oscillation, tropical cyclones, and deep convective cloud systems, similar to those using higher resolution in some degree (e.g., 3.5 and 7 km) (Kajikawa et al., 2016; Kikuchi et al., 2017; Kubokawa et al., 2012; Miura et al., 2007; Tomita et al., 2005).

We employ the 3-D snapshots of specific cloud water, cloud ice, rainwater, snow, and graupel contents with a 6-hr interval from the NICAM simulations. The convective cloud pixels are identified by using a threshold of condensed water mixing ratio greater than 10^{-5} kg·kg⁻¹ (Dauhut et al., 2015) and the cloud field should be at least 10 km uninterrupted from the cloud top downward with surface rainfall. Considering the model vertical resolution and boundaries of the TTL with a base at ~14.5 and top at ~18.5 km (Fu et al., 2007; Fueglistaler et al., 2009), the NICAM-simulated convective cloud fields with cloud top heights exceeding 15.5, 16.9, and 18.4 km (i.e., the 3 consecutive model levels) are analyzed to examine ODCs that reaches the TTL and the lower stratosphere. The consecutive ODC pixels are grouped together, which is considered as one ODC in our analyses. We also derive the cold point tropopause (CPT) temperature and height from the monthly mean temperature. The number of ODCs with top exceeding the CPT height is derived by interpolation based on a linear relation between ODC number and $\log(z)$. We consider the tropics between 20°N and 20°S, and six $10^{\circ} \times 10^{\circ}$ sub-regions along the equator, namely, over Pacific, Atlantic, and Indian Oceans, and over Amazon, Africa, and Maritime Continents (see Figure 1b). The water vapor mixing ratio, relative humidity (RH), and temperatures at 2 m are employed to derive the near-surface water vapor and temperature changes. The global near-surface temperature trend is used to scale the change in the occurrence and characteristics of ODCs in response to global warming.

The TRMM satellite (Kummerow et al., 1998, 2000), in operation from 1997 to 2015, provides valuable observational data for studying the distribution and variability of precipitation and convection over the tropics. The TRMM database (C. Liu et al., 2008) for the years 1998–2013 from the University of Utah

WU ET AL. 2 of 10

1944/8007, 2023, 14, Downloaded from https://auguubs.onlinelibrary.wiley.com/doi/10.1029/2023GL104210, Wiley Online Library on [27/07/2023]. See the Terms and Conditions (https://onlinelibrary.wiley.com/terms-and-conditions) on Wiley Online Library for rules of use; OA articles are governed by the applicable Creative Commons Licens

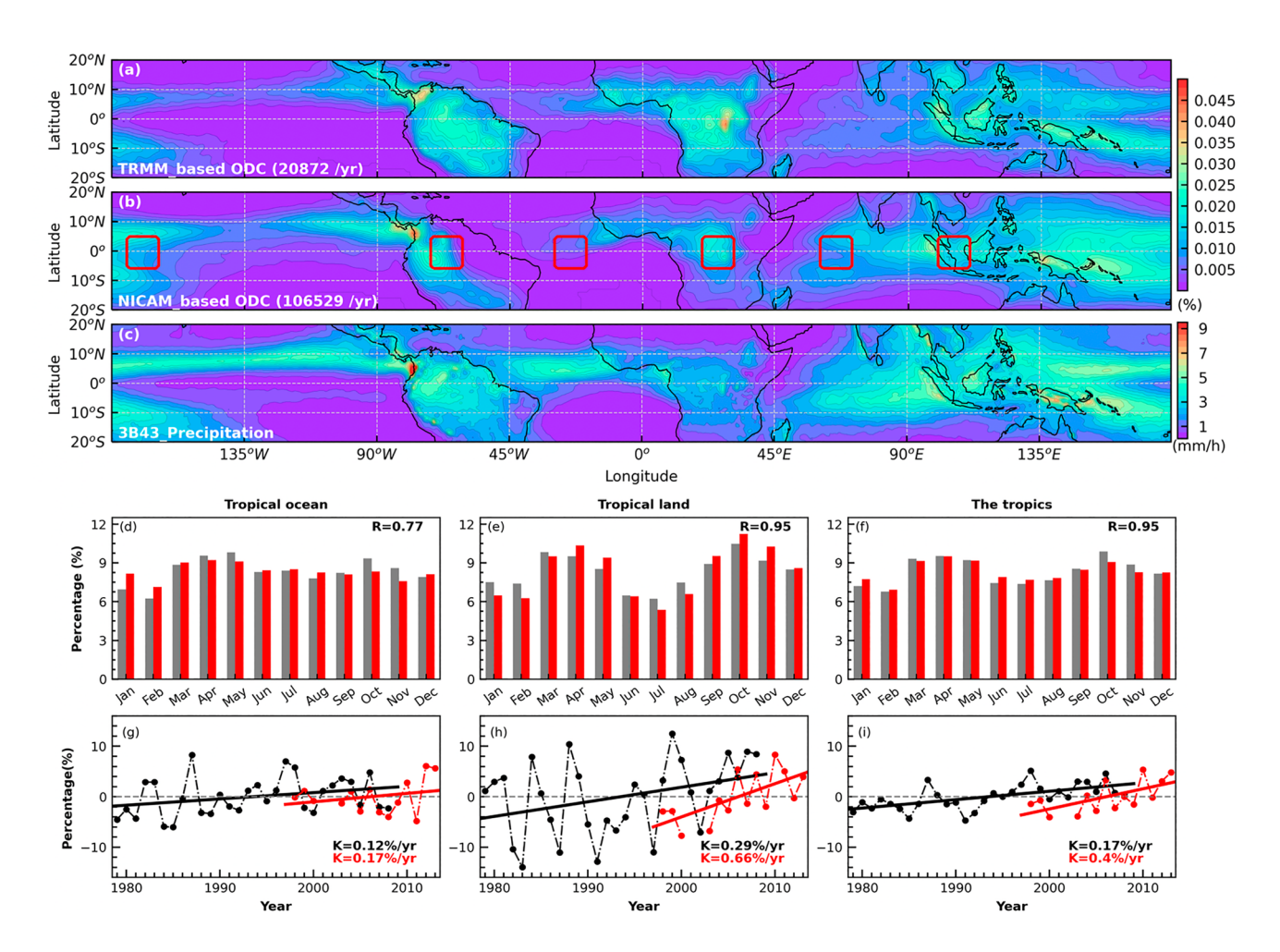


Figure 1. Comparison of Nonhydrostatic Icosahedral Atmosphere Model (NICAM) simulations with observations for 1998–2008. The upper three panels show geographical distribution climatology of (a) normalized occurrence frequency (%) of Tropical Rainfall Measuring Mission (TRMM)-observed overshooting deep convection (ODC) with minimum 10.8 μ m brightness temperature \leq 205 K, (b) normalized occurrence frequency (%) of NICAM-simulated ODC for cloud top height reaching above 15.5 km altitude, and (c) precipitation (mm/hr) from TRMM in the tropics for 1998–2008. The horizontal resolution is 1° × 1° for ODCs and the normalized occurrence frequency is the number of ODCs in each 1° × 1° grid divided by the total number over tropics (20°S–20°N). The numbers in the parentheses are average annual total numbers of ODC occurrences sampled by TRMM and NICAM. The horizontal resolution for precipitation is 0.25° × 0.25°. The lower two panels show temporal variations of the ODC as observed by TRMM (red color) and simulated by NICAM (black color). Bar plots (fourth row) show the seasonal cycle climatology of normalized ODC occurrence frequencies (%) defined as the ODC number in a given month divided by the total number for 1998–2008 over (d) Tropical ocean, (e) Tropical land, and (f) Tropics between 20°N and 20°S. The corresponding interannual variation of normalized ODC occurrence frequency defined as the yearly ODC number minus their average value and then divided by the average value is shown in panels (g–i). R in (d–f) is the correlation coefficients and K in (g–i) is the slopes of the fitting.

(http://atmos.tamucc.edu/trmm/data/) is adopted to show the spatial and temporal variations of observed deep convection and evaluate the NICAM simulation. The observed orbit data were grouped first into radar projection precipitation features (RPPFs) by considering the area of ground projection of radar reflectivity greater than or equal to 20 dBZ (C. Liu et al., 2008; Nesbitt et al., 2000). Considering a close relationship between convective cloud top temperature based on 10.8 μ m infrared brightness temperature (BT₁₁) and cloud top height (Aumann & Ruzmaikin, 2013; Aumann et al., 2018; Gettelman et al., 2002; C. Liu et al., 2007; Young et al., 2012), the RPPFs with BT₁₁ \leq 205 K are identified as TRMM-based ODCs, which roughly corresponds to the NICAM-based ODCs with cloud top height exceeding 15.5 km. The TRMM observed ODCs during the overlapping period (1998–2008) with the NICAM historical simulation are used to evaluate the NICAM-simulated ODCs, and the longer period is used to show the interannual variation and changes in observed ODCs for 1998–2013. We exclude 3 months including August 2001, September 2002, and October 2002 from the analysis because of data quality issues (Zipser et al., 2006).

The fractional change of tropical ODC frequency per K of global warming in the future climate is calculated from

WU ET AL. 3 of 10

articles are governed by the applicable Creative Co

$$\frac{(V_f - V_h)/V_h}{T_f - T_h}$$

which has units of %/K. In above equation, V is the ODC frequency, T is the near-surface air temperature (K). V and T are the averages over the historical (subscript h) and future (subscript f) periods. While V is an average over the regions considered, T is the average over the globe.

3. Comparison of NICAM-Derived ODCs With TRMM Observations

The spatiotemporal characteristics of tropical ODCs based on the TRMM observation and NICAM simulation in their overlapping period (1998–2008) are examined (Figure 1). Considering the distinct difference in ODC sampling between TRMM (20,872) and NICAM (106,529 yr⁻¹), the normalized spatial distribution of the tropical ODCs is compared. The spatial distributions of tropical ODCs from TRMM (Figure 1a) reveals that they are widespread over ocean but much more dense over land, which are mainly concentrated over the South America, tropical Africa, maritime continent, and the vast Indo-Pacific warm pool. The NICAM simulation (Figure 1b) reasonably reproduced observed spatial distribution of the ODCs in the tropics, which also overall agrees well with the CloudSat observations (Takahashi & Luo, 2014). The spatial correlation coefficient between Figures 1b and 1a is 0.71 that is statistically significant at 99% confidence level. The distribution pattern of tropical precipitation from TRMM (Figure 1c) shows the heaviest rain belt associated with the Intertropical Convergence Zone (ITCZ, Y. Liu et al., 2015). By comparison, it can be seen that the simulated ODC spatial pattern falls between the patterns of observed ODCs and precipitation (Figures 1a and 1c).

Figures 1a and 1b also indicate that NICAM tends to underestimate the ODC frequencies over land but overestimate them over ocean as compared with observations, leading to a proportion of 73.7% over ocean and 26.3% over land from NICAM versus 53.2% over ocean and 46.8% over land from TRMM. For example, over the Indian-Pacific warm pool, the NICAM has simulated the spatial distribution of ODCs reasonably well but with a larger magnitude than observation. The tropical Africa is known as the most active region on Earth for the most intense thunderstorms and lightning flashes (Cecil et al., 2014; C. Liu & Zipser, 2015; Wu et al., 2020; Zipser et al., 2006). The simulated main ODC location coincides well with the observations there, but both the coverage and magnitude of simulated ODCs are smaller than the observations. In addition, there is a notable difference in the northeastern region of South America, where almost no ODCs appear in the NICAM simulation. The differences between the simulation and observation indicate a need for further improvements of the GCRM simulations. The fact that simulated ODC spatial pattern falls between observed ODC and precipitation patterns (Figures 1a–1c) might suggest that the differences between simulated and observed ODCs can be partly caused by the different ODC definitions for TRMM observation and NICAM simulations. More importantly, although ODCs plays an important role in global rainfall, it might not dominate the distribution of precipitation, especially over the ocean where their inconsistency is more pronounced (Figures 1a and 1c).

Figures 1d–1f further confirm NICAM's capability to simulate deep convection by well reproducing observed seasonal variations of ODCs over ocean, land, and the entire tropics. Both simulations and observations show double peaks in boreal Spring and Autumn over land and similar seasonality over ocean but with much weaker peaks. The corresponding correlation coefficients for the ODC climatology annual cycle are 0.77, 0.95, and 0.95 over ocean, land, and tropics, respectively. The monthly time series of ODC frequency during the overlapping period (1998.01–2008.12) also have a strong positive correlation of 0.46, 0.65, and 0.72 which are all statistically significant at a 99% confidence level. Figures 1g–1i further shows the ODC inter-annual variation from NICAM for 1979–2008 and from TRMM for 1998–2013. The ODC yearly time series from NICAM shows positive trends for 1979–2008, and so do the TRMM time series for 1998–2013. It is interesting to notice that the trends from NICAM and TRMM are remarkably similar over oceans (Figure 1g) although they are for different periods. Both NICAM-simulated and the TRMM-observed ODCs show that tropical ODCs increase at a faster rate over land than over oceans.

4. Future Changes in Tropical ODCs

We next examine changes in tropical ODCs with cloud top height (CTH) exceeding 15.5, 16.9, and 18.4 km, noted as ODC_15.5km, ODC_16.9km, and ODC_18.4km. Figure 2 shows the spatial distributions of annual

WU ET AL. 4 of 10

19448007, 2023, 14, Downloaded from https://agupubs.onlinelibrary.wiley.com/doi/10.1029/2023GL104210, Wiley Online Library.on [27/07/2023]. See the Terms and Conditions

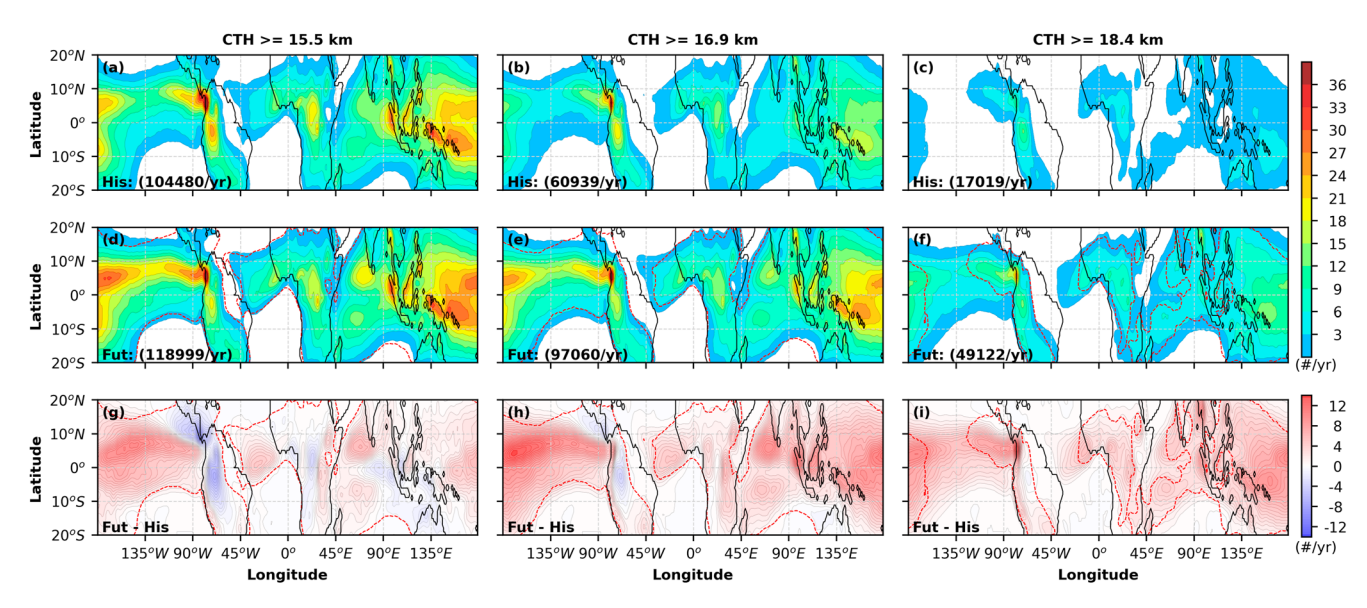


Figure 2. The spatial distribution of Nonhydrostatic Icosahedral Atmosphere Model-simulated overshooting deep convection (ODC) annual number (#/year) with a horizontal resolution of $1^{\circ} \times 1^{\circ}$ for different cloud top height, averaged over 1979–2008 (upper row), over 2075–2104 (middle row), and their difference (bottom row). The numbers in the parentheses are climatology annual total numbers of ODC occurrences over tropics. The red contour lines in the panels in the middle and bottom rows show the boundary of ODCs for 1979–2008.

ODC occurrence number for NICAM-simulated ODC_15.5km (left column), ODC_16.9km (middle column), and ODC_18.4km (right column) in the tropics for 1979–2008 (top row), 2075–2104 (middle row), and their differences (bottom row). More ODCs are distributed over the ocean, with the most frequent ODCs distributed in Indo-Pacific warm pool. The annual total occurrence of ODC_15.5km over the tropics will increase by 13.9% from 1979–2008 to 2075–2104. The increase mainly happens over the tropical ocean while the land area including tropical South America and Africa show a decrease (Figure 2g). Both the occurrence number and spatial extent of ODC_18.4km show dramatic increases in the future (Figures 2c, 2f, and 2i). The occurrence of ODC_18.4km will almost triple (and increase by 189%) by the end of this century, with an increase everywhere (Figure 2i). The future change in annual total ODC_16.9km occurrence is moderate (59.3%). Furthermore, the contributions of ODC_16.9km and ODC_18.4km occurrences to ODC_15.5km occurrences will rise from 58.3% to 16.3% in the historical period to 81.6% and 41.3% by the end of this century, respectively.

We further evaluate the changes in ODCs relative to the tropical cold-point tropopause (CPT) height that will increase with global warming (P. Lin et al., 2017; Lorenz & DeWeaver, 2007; Santer et al., 2003). The NICAM simulation shows an increasing trend in both CPT temperature and height in the tropics (Figure 3). From 1979–2008 to 2075–2104, the tropical mean CPT temperature and height will increase from 201.1 to 202.9 K, and 17.2 to 18.1 km, respectively. The most significant CPT height uplift zone is from the equatorial eastern Pacific to the Atlantic Ocean. The ODCs that penetrate the CPT height are shown in Figures 3c and 3f. The future annual tropical-average ODCs passing CPT height only shows a small increase of about 8% compared to historical periods, with a general increase over ocean but decrease on land (Figure 3i).

The formation of moist convection is directly associated with air temperature and moisture. The warmer the future atmosphere, the stronger the water-holding capacity, which is especially conducive to the formation of deep moist convection. Figure 4 shows the NICAM-projected near-surface (a) air temperature (T) and (b) water vapor mixing ratio (Q) in the tropics, together with Tables showing climatology and changes in temperature, water vapor mixing ratio, RH, and ODC occurrences over various regions. While the NICAM simulated global-mean surface air temperature increases by 2.67 K from historical period (1979–2008) to future period (2075–2104), the tropical-mean surface air temperature will increase by 2.60 K, with an increase of 3.68 K over land and an increase of 2.26 K over the ocean. The increase of temperature is thus more pronounced over the land than over the ocean (e.g., Fu & Feng, 2014; Joshi et al., 2008; Manabe et al., 1992). The water vapor mixing ratio also increases but with a more pronounced increase over ocean than land. The increase of water mixing ratio is 2.7 g/kg over the tropical ocean and 1.8 g/kg over tropical land. Note that while the RH generally increases over oceans,

WU ET AL. 5 of 10

1944/8007, 2023, 14, Downloaded from https://agupubs.onlinelibrary.wiley.com/doi/10.1029/2023GL104210, Wiley Online Library on [27/07/2023]. See the Terms and Conditions (https://onlinelibrary.wiley.com/terms-and-conditions) on Wiley Online Library for rules of use; OA articles are governed by the applicable Creative Commons Licensia.

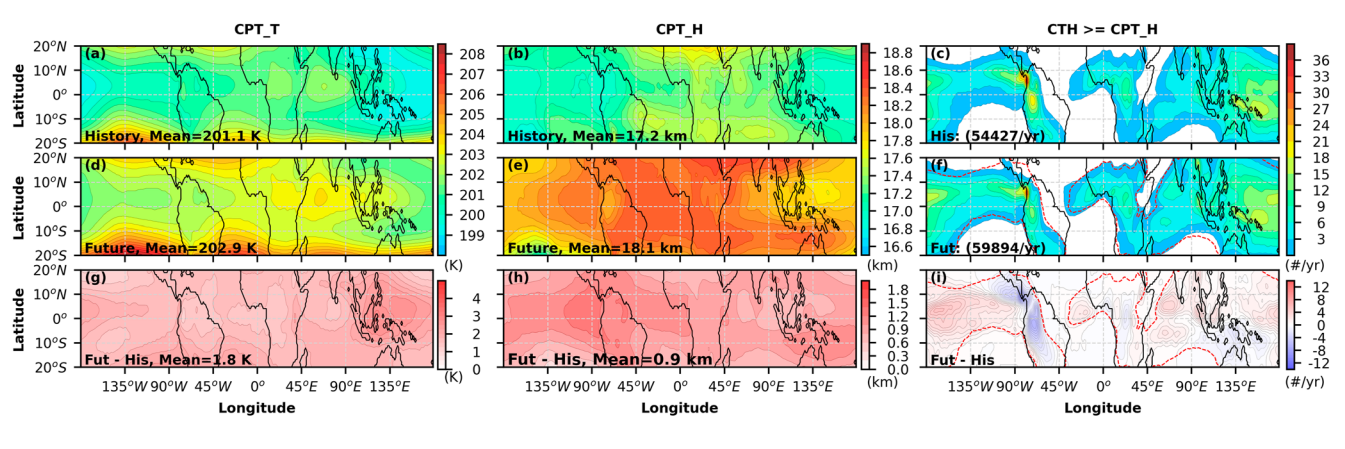


Figure 3. The spatial distribution of Nonhydrostatic Icosahedral Atmosphere Model-simulated tropical cold-point tropopause (CPT) temperature (CPT_T) (left), CPT height (CPT_H) (middle), and annual number of overshooting deep convection (ODC) with cloud top height reaching above CPT_H (right) with a horizontal resolution of $1^{\circ} \times 1^{\circ}$, averaged over the historical period of 1979–2008 (upper rows), over the future period of 2075–2104 (middle rows), and their differences (lower rows). The red dashed lines in panels (f, i) show the boundary of ODCs for 1979–2008 in panel (c).

it decreases over land in the future. The different changes in temperature and RH between land and ocean imply a future drying terrestrial climate (Fu & Feng, 2014; Sherwood & Fu, 2014).

The different near-surface atmospheric environments over land and ocean might be partly responsible for different responses of ODCs. In Tables in Figure 4, we show both ODC number percentage changes and those scaled by the global-mean temperature change over various regions. Over the tropical land, the numbers of ODC_16.9km and ODC_18.4km are predicted to increase by about 27% and 98% compared to the historical period, corresponding to

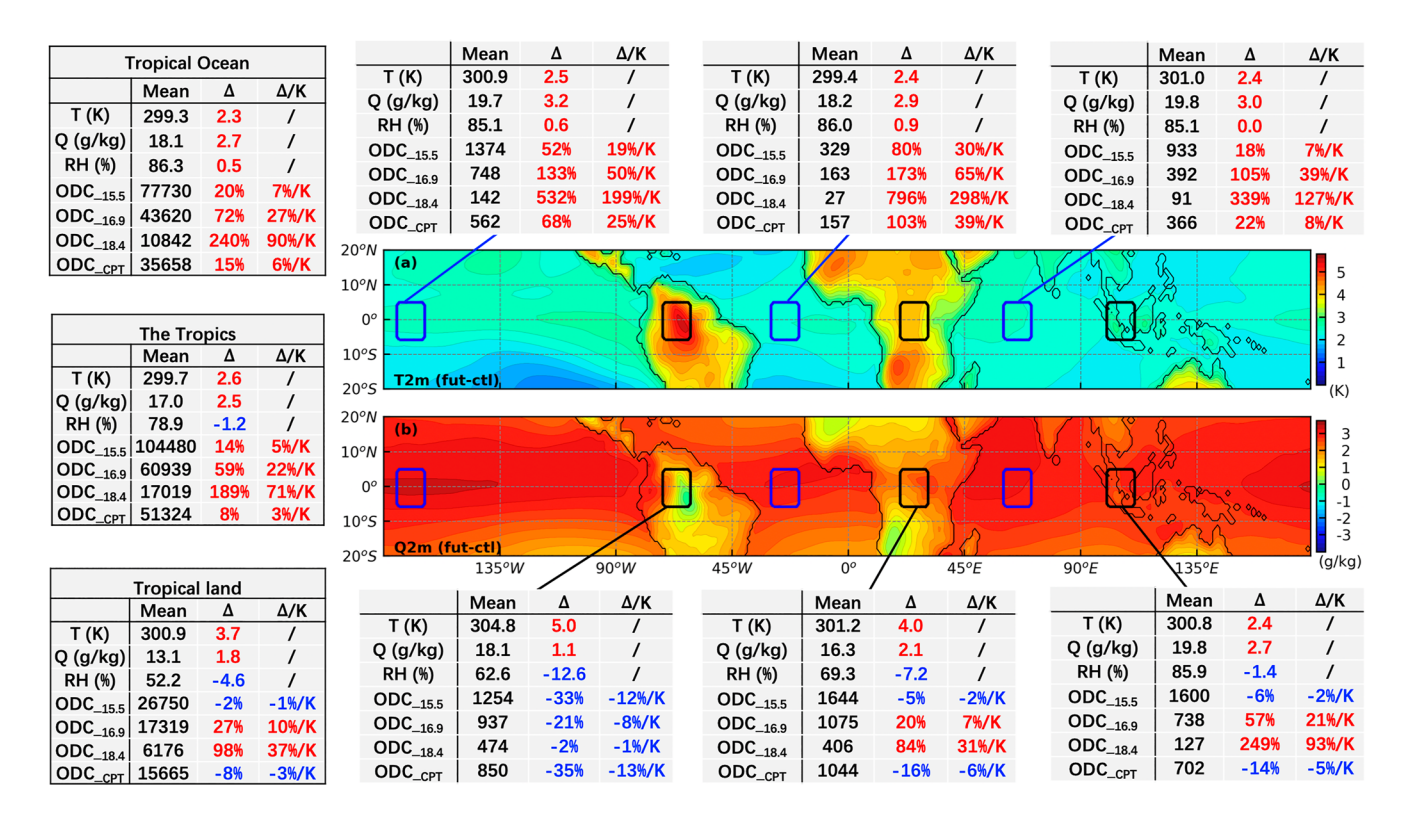


Figure 4. The spatial distribution of the Nonhydrostatic Icosahedral Atmosphere Model-simulated near-surface (a) air temperature (K) and (b) water vapor mixing ratio (g/kg) changes from the 1979–2008 to 2075–2104, along with the tables showing climatology (Mean) for 1979–2008 and future changes (Δ) of temperature (T), water vapor mixing ratio (Q), relative humidity, and overshooting deep convection (ODC) occurrences (the ODC occurrence changes are denoted as the percentage changes), and ODC occurrence percentage changes scaled by global mean temperature changes (2.67 K) (Δ/K), over different tropical regions. Red (blue) color in tables represent increasing (decreasing) changes.

WU ET AL. 6 of 10

the percentage changes per degree warming by 10%/K and 37%/K. For ODC_15.5km, it is predicted to decrease slightly, by about -2% (-1%/K). Over the wide tropical ocean, all three categories of ODCs (i.e., ODC_15.5km, ODC_16.9km, and ODC_18.4km) are predicted to increase, with percentage increase (rate) of 20% (7%/K), 72% (27%/K), and 240% (90%/K), respectively, much faster than those over land. If considering the percentage change rates with local mean air temperature (Finney et al., 2014; Romps et al., 2014), the differences between land and ocean would be even larger. For ODCs with CPT height as a reference level, the changes averaged over ocean and land are 15% (i.e., 6%/K) and -8% (i.e., -3%/K), respectively.

Some drastic changes are also seen over the six sub-regions along the equator (Figure 4). It is well known that precipitation events over the tropical ocean are dominated by heavy rainfall but weaker convective intensity and less lightning (Cecil et al., 2014; Qie et al., 2014; Zipser et al., 2006). The density of ODCs (i.e., ODC numbers within $1^{\circ} \times 1^{\circ}$ grid box) over the oceanic regions is generally less than that in continental regions in the historical period, especially those associated with ODC_16.9km and ODC_18.4km (in Figure 2). However, the increase rates with global warming over ocean are much faster than over land regions. The strong increase in atmospheric water vapor mixing ratio (atmospheric water content) and moderate increase of air temperature over the ocean will lead to a significant moister future oceanic climate. As the results, the most significant increase of ODCs (i.e., ODC_18.4km) appears over the Atlantic (796.3%/K and 298.2%/K), followed by the Pacific (531.7%/K and 199.1%/K). In contrast, a large increase in air temperature and a weak increase in atmospheric water vapor content over land will lead to a large decrease in RH and thus a drier future terrestrial climate. The ODCs over tropical land shows a decrease in total number for ODC 15.5km but still an increase in ODCs with higher cloud top height of ODC 16.9km, and ODC_18.4km. The terrestrial climate drying is most pronounced in the central South America (Feng & Fu, 2013), where the temperature rises by 5.0 K but the mixing ratio only increases by 1.1 g/kg, leading to a large decrease in RH (-12.6%), where all three types of ODCs are predicted to decrease. This is followed by Africa with increases of 4.0 K and 2.1 g/kg, and the predicted trends of ODCs are similar to the tropical land averages. The wide Indo-Pacific Warm Pool, due to the unique geography and circulation characteristics, is the region that contributes the most to ODCs in the tropics. The ODC in this area not only has a high density and a vast distribution extent but also has a much faster increase rate for ODC_16.9km, and ODC_18.4km than tropical land average, which is even comparable to the increase rate averaged over the tropical oceans. The ODC numbers for ODC_15.5km will decrease in the future over all three sub-land regions. For ODCs with CPT height as a reference level, ODC decreases in all sub-land regions with the largest future reduction over the South America by -35% (i.e., -13%/K).

5. Conclusions and Discussion

Overshooting deep convection has the ability to vertically transport pollutants especially short-lived chemicals rapidly into the TTL and lower stratosphere, which has important implications for stratospheric ozone and global climate. The tropics is well-known as the region with the most frequent intense storms and lightning on Earth (Cecil et al., 2014; Wu et al., 2020; Zipser et al., 2006). The present study is the first to examine climatology characteristics of tropical ODCs and how tropical ODCs change in response to a future warmer climate by using the global atmospheric model with explicit cloud microphysics. The NICAM simulations well reproduce the spatiotemporal characteristics of tropical ODCs observed by the TRMM satellite.

Based on the 30-year long-term NICAM simulations both on historical (1979–2008) and future (2075–2104) periods, it is found that the predicted tropical ODC occurrences with different cloud top heights generally show increasing trends, and that the higher the cloud top height, the greater the relative increase in the occurrence frequency. Specifically, ODCs with CTH reaching above 15.5 km will increase by 14% by the end of this century but the ODCs with CTH reaching 18.4 km almost triple in comparison with the historical period. This is consistent with recent results of the predicted increases in extreme heavy precipitation from NICAM and CMIP6 models (Na et al., 2020). The NICAM predicts that the future warmer climate will be drier over land and wetter over oceans. A warmer and wetter atmosphere over ocean is conducive to the growth of moist convection to higher heights. This ultimately results in a multiplied increase in the occurrence frequency of ODCs over the ocean. For example, ODCs with CTH reaching 18.4 km increase by 339%, 532%, and 796% over the tropical Indian, Pacific, and Atlantic Oceans. For tropical land, a hotter and drier future climate will lead to a relatively weak increase (and even a slight decrease for ODCs with CTH 15.5 km) of deep convection frequency.

The future tropical ODC occurrences show much larger relative increases for higher ODCs and much larger relative increases over ocean than over land. But this does not portent a much stronger vertical transport passing the

WU ET AL. 7 of 10

CPT that will increase with global warming. Relative to tropical CPT, ODCs will increase by only 8% with 15% over ocean but decrease by -8% over land. Finally it is noted that both the horizontal and vertical resolutions in this study might still be too coarse to accurately resolve deep convection, which should be further investigated and validated with "K-scale" models (e.g., Slingo et al., 2022).

Data Availability Statement

The data of TRMM observations can be found from the University of Utah TRMM Precipitation Feature Database at http://atmos.tamucc.edu/trmm/data/. The terms and guideline of NICAM data can be accessed online from http://nicam.jp/hiki Research + Collaborations. All the NICAM runs were performed on the K computer at the RIKEN Advanced Institute for Computational Science (Proposal number hp120279, hp130010, and hp140219).

Acknowledgments

This research was jointly sponsored by the National Natural Science Foundation of China (42275068 and 42130601) and China Scholarship Council (201906185035). It was also in part supported by NSF Grant AGS-2202812. The authors are grateful to Dr. Chuntao Liu for his assistance in clustering cloud field from NICAM simulations.

References

- Aumann, H. H., Behrangi, A., & Wang, Y. (2018). Increased frequency of extreme tropical deep convection: AIRS observations and climate model predictions. Geophysical Research Letters, 45(24), 13530-13537. https://doi.org/10.1029/2018GL079423
- Aumann, H. H., & Ruzmaikin, A. (2013). Frequency of deep convective clouds in the tropical zone from 10 years of AIRS data. Atmospheric Chemistry and Physics, 13(21), 10795-10806. https://doi.org/10.5194/acp-13-10795-2013
- Ban, N., Schmidli, J., & Schär, C. (2015). Heavy precipitation in a changing climate: Does short-term summer precipitation increase faster? Geophysical Research Letters, 42(4), 1165-1172. https://doi.org/10.1002/2014GL062588
- Bao, J., Sherwood, S. C., Alexander, L. V., & Evans, J. P. (2017). Future increases in extreme precipitation exceed observed scaling rates. Nature Climate Change, 7(2), 128–132. https://doi.org/10.1038/nclimate3201
- Bergman, J., Jensen, E., Pfister, L., & Yang, Q. (2012). Seasonal differences of vertical-transport efficiency in the tropical tropopause layer: On the interplay between tropical deep convection, large-scale vertical ascent, and horizontal circulations. Journal of Geophysical Research, 117(D5), D05302, https://doi.org/10.1029/2011JD0
- Cecil, D. J., Buechler, D. E., & Blakeslee, R. J. (2014). Gridded lightning climatology from TRMM-LIS and OTD: Dataset description. Atmospheric Research, 135-136(1), 404-414. https://doi.org/10.1016/j.atmosres.2012.06.028
- Chaboureau, J.-P., Cammas, J.-P., Duron, J., Mascart, P. J., Sitnikov, N. M., & Voessing, H.-J. (2007). A numerical study of tropical cross-tropopause transport by convective overshoots. Atmospheric Chemistry and Physics, 7, 1731-1740. https://doi.org/10.5194/acp-7-1731-2007
- Dauhut, T., Chaboureau, J.-P., Escobar, J., & Mascart, P. (2015). Large-eddy simulations of hector the convector making the stratosphere wetter. Atmospheric Science Letters, 16(2), 135-140. https://doi.org/10.1002/asl2.534
- Del Genio, A. D., Yao, M.-S., & Jonas, J. (2007). Will moist convection be stronger in a warmer climate? Geophysical Research Letters, 34(16), L16703, https://doi.org/10.1029/2007GL030525
- Donat, M. G., Lowry, A. L., Alexander, L. V., O'Gorman, P. A., & Maher, N. (2016). More extreme precipitation in the world's dry and wet regions. Nature Climate Change, 6(2), 508-513. https://doi.org/10.1038/nclimate3160
- Fan, J., Comstock, J. M., Ovchinnikov, M., McFarlane, S. A., McFarquhar, G., & Allen, G. (2010). Tropical anvil characteristics and water vapor of the tropical tropopause layer: Impact of heterogeneous and homogeneous freezing parameterizations. Journal of Geophysical Research, 115(D12), D12201. https://doi.org/10.1029/2009JD012696
- Feng, S., & Fu, Q. (2013). Expansion of global drylands under a warming climate. Atmospheric Chemistry and Physics, 13(19), 10081–10094. https://doi.org/10.5194/acp-13-10081-2013
- Finney, D. L., Doherty, R. M., Wild, O., Huntrieser, H., Pumphrey, H. C., & Blyth, A. M. (2014). Using cloud ice flux to parametrize large-scale lightning. Atmospheric Chemistry and Physics, 14(23), 12665-12682. https://doi.org/10.5194/acp-14-12665-2014
- Frey, W., Schofield, R., Hoor, P., Kunkel, D., Ravegnani, F., Ulanovsky, A., et al. (2015). The impact of overshooting deep convection on local transport and mixing in the tropical upper troposphere/lower stratosphere (UTLS). Atmospheric Chemistry and Physics, 15(11), 6467-6486. https://doi.org/10.5194/acp-15-6467-2015
- Fu, Q., & Feng, S. (2014). Responses of terrestrial aridity to global warming. Journal of Geophysical Research: Atmospheres, 119(13), 7863-7875, https://doi.org/10.1002/2014JD021608
- Fu, Q., Hu, Y. X., & Yang, Q. (2007). Identifying the top of the tropical tropopause layer from vertical mass flux analysis and CALIPSO lidar cloud observations. Geophysical Research Letters, 34(14), L14813. https://doi.org/10.1029/2007GL030099
- Fueglistaler, S., Dessler, A. E., Dunkerton, T. J., Folikins, I., Fu, Q., & Mote, P. W. (2009). Tropical tropopause layer. Reviews of Geophysics, 47(1), RG1004. https://doi.org/10.1029/2008RG000267
- Gettelman, A., Salby, M. L., & Sassi, F. (2002). Distribution and influence of convection in the tropical tropopause region. Journal of Geophysical Research, 107(D10), ACL6-1-ACL6-12. https://doi.org/10.1029/2001JD001048
- Grosvenor, D. P., Choularton, T. W., Coe, H., & Held, G. (2007). A study of the effect of overshooting deep convection on the water content of the TTL and lower stratosphere from Cloud Resolving Model simulations. Atmospheric Chemistry and Physics, 7(18), 4977–5002. https://doi. org/10.5194/acp-7-4977-2007
- Joshi, M. M., Gregory, J. M., Webb, M. J., Sexton, D. M. H., & Johns, T. C. (2008). Mechanisms for the land/sea warming contrast exhibited by simulations of climate change. Climate Dynamics, 30(5), 455-465. https://doi.org/10.1007/s00382-007-0306-1
- Kajikawa, Y., Miyamoto, Y., Yoshida, R., Yamaura, T., Yashiro, H., & Tomita, H. (2016). Resolution dependence of deep convections in a global simulation from over 10-kilometer to sub-kilometer grid spacing. Progress in Earth and Planetary Science, 3(1), 16. https://doi.org/10.1186/ s40645-016-0094-5
- Kikuchi, K., Kodama, C., Nasuno, T., Nakano, M., Miura, H., Satoh, M., et al. (2017). Tropical intraseasonal oscillation simulated in an AMIPtype experiment by NICAM. Climate Dynamics, 48(7-8), 2507-2528. https://doi.org/10.1007/s00382-016-3219-z
- Kodama, C., Yamada, Y., Noda, A. T., Kikuchi, K., Kajikawa, Y., Nasuno, T., et al. (2015). A 20-year climatology of a NICAM AMIP-type simulation. Journal of the Meteorological Society of Japan Series II, 93(4), 393-424. https://doi.org/10.2151/jmsj.2015-024
- Kuang, Z. M., & Bretherton, C. S. (2004). Convective influence on the heat balance of the tropical tropopause layer: A cloud-resolving model study. Journal of the Atmospheric Sciences, 61(23), 2919-2927. https://doi.org/10.1175/JAS-3306.1

WU ET AL. 8 of 10



Geophysical Research Letters

- 10.1029/2023GL104210
- Kubokawa, H., Fujiwara, M., Nasuno, T., Miura, M., Yamamoto, M. K., & Satoh, M. (2012). Analysis of the tropical tropopause layer using the nonhydrostatic icosahedral atmospheric model (NICAM): 2. An experiment under the atmospheric conditions of December 2006 to January 2007. Journal of Geophysical Research, 117(D17), D17114. https://doi.org/10.1029/2012JD017737
- Kummerow, C., Barnes, W., Kozu, T., Shiue, J., & Simpson, J. (1998). The tropical rainfall measuring mission (TRMM) sensor package. *Journal of Atmospheric and Oceanic Technology*, 15(3), 809–817. https://doi.org/10.1175/1520-0426(1998)015,0809:TTRMMT.2.0.CO;2
- Kummerow, C., Simpson, J., Thiele, O., Barnes, W., Chang, A. T. C., Stocker, E., et al. (2000). The status of the Tropical Rainfall Measuring Mission (TRMM) after two years in orbit. *Journal of Applied Meteorology and Climatology*, 39(12), 1965–1982. https://doi.org/10.1175/1520-0450(1998)015<0809:TTRMMT>2.0.CO;2
- Küpper, C., Thuburn, J., Craig, G. C., & Birner, T. (2004). Mass and water transport into the tropical stratosphere: A cloud-resolving simulation. *Journal of Geophysical Research*, 109(D10), D10111. https://doi.org/10.1029/2004JD004541
- Lin, L., Wang, Z., Xu, Y., & Fu, Q. (2016). Sensitivity of precipitation extremes to radiative forcing of greenhouse gases and aerosols. Geophysical Research Letters, 43(18), 9860–9868. https://doi.org/10.1002/2016GL070869
- Lin, L., Wang, Z., Xu, Y., Fu, Q., & Dong, W. (2018). Larger sensitivity of precipitation extremes to aerosol than greenhouse gas forcing in CMIP5 models. *Journal of Geophysical Research: Atmospheres*, 123, 8062–8073. https://doi.org/10.1029/2018JD028821
- Lin, P., Paynter, D., Ming, Y., & Ramaswamy, V. (2017). Changes of the tropical tropopause layer under global warming. *Journal of Climate*, 30(4), 1245–1258. https://doi.org/10.1175/JCLI-D-16-0457.1
- Liu, C. (2017). Severe weather in a warming climate. Nature, 544(7651), 422-423. https://doi.org/10.1038/544422a
- Liu, C., & Zipser, E. J. (2015). The global distribution of largest, deepest, and most intense precipitation systems. Geophysical Research Letters, 42(9), 3591–3595. https://doi.org/10.1002/2015GL063776
- Liu, C., Zipser, E. J., Cecil, D. J., Nesbitt, S. W., & Sherwood, S. (2008). A cloud and precipitation feature database from nine years of TRMM observations. *Journal of Applied Meteorology and Climatology*, 47(10), 2712–2728. https://doi.org/10.1175/2008JAMC1890.1
- Liu, C., Zipser, E. J., & Nesbitt, S. W. (2007). Global distribution of tropical deep convection: Different perspectives from TRMM infrared and radar data. *Journal of Climate*, 20(3), 489–503. https://doi.org/10.1175/JCLI4023.1
- Liu, Y., Li, L., Shi, Z., Wei, K. Y., Chou, C. J., Chen, Y. C., et al. (2015). Obliquity pacing of the western Pacific intertropical convergence zone over the past 282,000 years. *Nature Communications*, 6(1), 10018. https://doi.org/10.1038/ncomms10018
- Lorenz, D. J., & DeWeaver, E. T. (2007). Tropopause height and zonal wind response to global warming in the IPCC scenario integrations. *Journal of Geophysical Research*, 112(D10), D10119. https://doi.org/10.1029/2006JD008087
- Manabe, S., Spelman, M. J., & Stouffer, R. J. (1992). Transient responses of a coupled ocean-atmosphere model to gradual changes of atmospheric CO₂. Part II: Seasonal response. *Journal of Climate*, 5(2), 105–126. https://doi.org/10.1175/1520-0442(1991)004<0785:TROACO>
- Min, S.-K., Zhang, X., Zwiers, F. W., & Hegerl, G. C. (2011). Human contribution to more-intense precipitation extremes. *Nature*, 470(7334), 378–381. https://doi.org/10.1038/NATURE09763
- Miura, H., Satoh, M., Nasuno, T., Noda, A. T., & Oouchi, K. (2007). A Madden–Julian oscillation event realistically simulated by a global cloud-resolving model. *Science*, 318(5857), 1763–1765. https://doi.org/10.1126/science.1148443
- Na, Y., Fu, Q., & Kodama, C. (2020). Precipitation probability and its future changes from a global cloud-resolving model and CMIP6 simulations. *Journal of Geophysical Research: Atmospheres*, 125(5), e2019JD031926. https://doi.org/10.1029/2019JD031926
- Na, Y., Fu, Q., Leung, L. R., Kodama, C., & Lu, R. (2022). Mesoscale convective systems simulated by a high-resolution global nonhydro-static model over the United States and China. *Journal of Geophysical Research: Atmospheres*, 127(7), e2021JD035916. https://doi.org/10.1029/2021JD035916
- Nesbitt, S. W., Zipser, E. J., & Cecil, D. J. (2000). A census of precipitation features in the tropics using TRMM: Radar, ice scattering, and light-ning observations. *Journal of Climate*, 13(23), 4087–4106. https://doi.org/10.1175/1520-0442(2000)013<4087;ACOPFI>2.0.CO;2
- O'Gorman, P. A. (2015). Precipitation extremes under climate change. Current Climate Change Reports, 1(2), 49–59. https://doi.org/10.1007/s40641-015-0009-3
- O'Gorman, P. A., & Schneider, T. (2009). The physical basis for increases in precipitation extremes in simulations of 21st-century climate change. *Proceedings of the National Academy of Sciences of the United States of America*, 106(35), 14773–14777. https://doi.org/10.1073/pnas.0907610106
- Pan, L. L., Atlas, E. L., Salawitch, R. J., Honomichl, S. B., Bresch, J. F., Randel, W. J., et al. (2017). The convective transport of active species in the tropics (CONTRAST) experiment. Bulletin of the American Meteorological Society, 98(1), 106–128. https://doi.org/10.1175/ BAMS-D-14-00272.1
- Qie, X., Wu, X., Yuan, T., Bian, J., & Lu, D. (2014). Comprehensive pattern of deep convective systems over the Tibetan Plateau-South Asian monsoon region based on TRMM data. *Journal of Climate*, 27(17), 6612–6626. https://doi.org/10.1175/JCLI-D-14-00076.1
- Romps, D. M. (2019). Evaluating the future of lightning in cloud-resolving models. Geophysical Research Letters, 46(24), 14863–14871. https://doi.org/10.1029/2019GL085748
- Romps, D. M., Seeley, J. T., Vollaro, D., & Molinari, J. (2014). Projected increase in lightning strikes in the United States due to global warming. Science, 346(6211), 851–854. https://doi.org/10.1126/science.1259100
- Santer, B. D., Sausen, R., Wigley, T. M. L., Boyle, J. S., AchutaRao, K., Doutriaux, C., et al. (2003). Behavior of tropopause height and atmospheric temperature in models, reanalyses, and observations: Decadal changes. *Journal of Geophysical Research*, 108(D1), ACL1-1–ACL1-22. https://doi.org/10.1029/2002JD002258
- Satoh, M., Matsuno, T., Tomita, H., Miura, H., Nasuno, T., & Iga, S. (2008). Nonhydrostatic Icosahedral Atmospheric Model (NICAM) for global cloud resolving simulations. *Journal of Computational Physics*, 227(7), 3486–3514. https://doi.org/10.1016/j.jcp.2007.02.006
- Satoh, M., Stevens, B., Judt, F., Khairoutdinov, M., Lin, S., Putman, W. M., & Düben, P. (2019). Global cloud-resolving models. *Current Climate Change Reports*, 5(3), 172–184. https://doi.org/10.1007/s40641-019-00131-0
- Satoh, M., Tomita, H., Yashiro, H., Miura, H., Kodama, C., Seiki, T., et al. (2014). The non-hydrostatic icosahedral atmospheric model: Description and development. *Progress in Earth and Planetary Science*, 1(1), 18. https://doi.org/10.1186/s40645-014-0018-1
- Satoh, M., Yamada, Y., Sugi, M., Kodama, C., & Noda, A. T. (2015). Constraint on future change in global frequency of tropical cyclones due to global warming. *Journal of the Meteorological Society of Japan Ser II*, 93(4), 489–500. https://doi.org/10.2151/jmsj.2015-025
- Sherwood, S., & Fu, Q. (2014). A drier future? Science, 343(6172), 737-739. https://doi.org/10.1126/science.1247620
- Slingo, J., Bates, P., Bauer, P., Belcher, S., Palmer, T., Stephens, G., et al. (2022). Ambitious partnership needed for reliable climate prediction. Nature Climate Change, 12(6), 499–503. https://doi.org/10.1038/s41558-022-01384-8
- Takahashi, H., & Luo, Z. J. (2014). Characterizing tropical overshooting deep convection from joint analysis of CloudSat and geostationary satellite observations. *Journal of Geophysical Research: Atmospheres*, 119(1), 112–121. https://doi.org/10.1002/2013JD020972

WU ET AL. 9 of 10

Geophysical Research Letters

- 10.1029/2023GL104210
- Taylor, C., Belušić, D., Guichard, F., Parker, D. J., Vischel, T., Bock, O., et al. (2017). Frequency of extreme Sahelian storms tripled since 1982 in satellite observations. *Nature*, 544(7651), 475–478. https://doi.org/10.1038/nature22069
- Tomita, H., Miura, H., Iga, S., Nasuno, T., & Satoh, M. (2005). A global cloud-resolving simulation: Preliminary results from an aqua planet experiment. *Geophysical Research Letters*, 32(8), L08805. https://doi.org/10.1029/2005GL022459
- Tomita, H., & Satoh, M. (2004). A new dynamical framework of nonhydrostatic global model using the icosahedral grid. *Fluid Dynamics Research*, 34(6), 357–400. https://doi.org/10.1016/j.fluiddyn.2004.03.003
- Tong, M., Zheng, Z., & Fu, Q. (2022). Evaluation of East Asian Meiyu from CMIP6/AMIP simulations. Climate Dynamics, 59(7–8), 2429–2444. https://doi.org/10.1007/s00382-022-06218-z
- Wu, X., Yuan, T., Kai, Q., & Luo, J. (2020). Geographical distribution of extreme deep and intense convective storms on Earth. *Atmospheric Research*, 235, 104789. https://doi.org/10.1016/j.atmosres.2019.104789
- Young, A. H., Bates, J. J., & Curry, J. A. (2012). Complementary use of passive and active remote sensing for detection of penetrating convection from CloudSat, CALIPSO, and Aqua MODIS. *Journal of Geophysical Research*, 117(D13), D13205. https://doi.org/10.1029/2011JD016749
- Zipser, E. J., Cecil, D. J., Liu, C. T., Nesbitt, S. W., & Yorty, D. P. (2006). Where are the most intense thunderstorms on Earth? *Bulletin of the American Meteorological Society*, 87(8), 1057–1071. https://doi.org/10.1175/BAMS-87-8-1057

WU ET AL. 10 of 10